

Ultrasound Contrast Plane Wave Imaging

Olivier Couture, Mathias Fink, and Mickael Tanter

Abstract—**Background:** Monitoring the accumulation of microbubbles within tissue vasculature with ultrasound allows both molecular and perfusion imaging. Unfortunately, conventional imaging with focused pulses can destroy a large fraction of the microbubbles it is trying to follow. Using coherent synthetic summation, ultrafast plane wave imaging could attain similar image quality, while reducing the peak acoustic pressure and bubble disruption. **Method:** In these experiments, microbubbles were flowed in a wall-less vessel phantom. Images were obtained on a programmable clinical scanner with a set of line-per-line focused pulses for conventional contrast imaging and with compounded plane wave transmission adapted for nonlinear imaging. Imaging was performed between 14 and 650 kPa peak negative pressure at 7.5 MHz. The disruption of the microbubbles was evaluated by comparing the microbubble intensity before and after acquisition of a set of 100 images at various pressures. **Results:** The acoustic intensity required to disrupt 50% of the microbubbles was 24 times higher with plane-wave imaging compared with conventional focused pulses. Although both imaging approaches yield similar resolution, at the same disruption level, plane-wave imaging showed better contrast. In particular, at similar disruption ratio (50% after 100 images), contrast-pulse sequencing (CPS) performed with plane waves displayed an improvement of 11 dB compared with conventional nonlinear imaging. **Conclusion:** In each resolution cell of the image, plane-wave imaging spread the spatial peak acoustic intensity over more pulses, reducing the peak pressure and, hence, preserving the microbubbles. This method could contribute to molecular imaging by allowing the continuous monitoring of the accumulation of microbubbles with improved contrast.

I. INTRODUCTION

THE presence of microbubbles causes a very large echo on ultrasound images because of their high scattering cross-section and resonance [1]. Additionally, their nonlinear acoustic response and propensity to disrupt [AU2: **What is meant by disrupt in this context?**] facilitate their detection with advanced pulse sequences [2]–[4]. Hence, a single bubble, 1 to 5 μm in diameter, flowing through a capillary can be detected with a clinical ultrasound scanner. The injection of ultrasound contrast agent is currently used to enhance contrast from blood and improve the visualization of the coronary chamber [5] and liver perfusion [6]. The exquisite sensitivity of ultrasound to its contrast agents also triggered the interest in their application to molecular imaging. By functionalizing microbubbles with antibodies or short peptides, it is possible

to enhance drastically their affinity to thrombus, arteriosclerotic plaque [7] and neovasculature [8] through specific biological targets.

The accumulation of microbubbles in a tumor through molecular interaction is a dynamic process [9]. After injection, the microbubbles flow through the entire vasculature and accumulate within neovasculature by attaching themselves to their target. Meanwhile, the free-flowing microbubbles are slowly eliminated by their passage through the lungs and the liver. After a 10 min waiting period, it is generally considered that the contrast enhancement is due to microbubbles targeted to the biomarker of interest. Meanwhile, the entire dynamic of microbubble specific uptake can yield helpful information because it is linked to total blood flow, blood volume, site-specificity, and ligand affinity [10]. To obtain estimates of these physiological parameters, images of the contrast agents should be taken at a fast rate and with sufficient contrast-to-tissue ratio.

However, microbubble imaging very often suffers from a quantum-mechanic-like conundrum, wherein the very detection of the contrast agents by the ultrasound scanner can induce their disappearance. Indeed, ultrasound contrast agents can be disrupted by acoustic waves at fairly low pressures, down to 300 kPa at 7.5 MHz [11], [12]. Unfortunately, these pressure levels are often required for their distinction from tissue. Because of the fragility of the microbubbles, sonographers generally must reduce the acoustic pressure and the frame-repetition frequency to a minimum (down to 1 image every 15 s with an MI = 0.25 at 7 MHz in Tardy *et al.* [8]) to preserve the contrast agents for functional imaging in slow flow conditions. This trade-off dramatically reduces the amount of information available in perfusion and molecular imaging with ultrasound. A solution to this unsatisfying compromise would require an imaging technique that preserves the contrast between the microbubble and the surrounding tissue while reducing the disruption induced by the imaging itself.

In the past decade, the concept of ultrafast imaging based on the successive transmissions of ultrasonic plane waves was introduced in the ultrasound community [13], [14]. Indeed, an image with a large field of view can be beamformed from a single plane wave if its echoes are recorded by a sufficient number of parallel reception channels. Such plane-wave imaging was first applied to transient elastography [13] and then to shear wave elastography in conjunction with acoustic radiation force pulses [15]. The combination of compounded plane wave transmissions was then introduced for ultrafast vector Doppler imaging [14] and recently for high-quality ultrafast B-mode imaging [16]. The application of plane wave compounding to blood flow measurements also led to ultrafast Doppler for cardiovascular applications and ultrasensitive Doppler [17]

Manuscript received April 10, 2012; accepted September 3, 2012.

O. Couture is with CNRS, Institut Langevin, Paris, France.

M. Fink is with Ecole Supérieure de Physique et de Chimie Industrielles de la Ville de Paris, Institut Langevin, Paris, France.

M. Tanter is with INSERM, Institut Langevin, Paris, France. [AU1: **Please spell out all abbreviations in affiliations.**]

DOI <http://dx.doi.org/TBC>

DRAFT

for functional brain imaging [18]. The research prototypes leveraged by our group in the last decade led to the development of an ultrasound research platform which is only limited by the delay to echo and can attain 20 000 frames per second. Such frame-rates, however, require numerous acquisition channels (typically 128) and the capacity to transfer and beamform hundreds of megabits per seconds. They are plagued by low SNR and contrast. Because all pixels of the image are interrogated by the same pulse, the acoustic energy is spread rather than focused. However, Montaldo *et al.* [16] have shown that the SNR and contrast can be retrieved by emitting plane waves at various angles and compounding the beamformed coherent images. With a limited number of plane waves, an image equivalent to focused imaging can be obtained. Moreover, because no transmit focusing is involved, the synthetic recombination of plane wave transmissions provides a virtual dynamic focusing in the transmit mode and the quality of the image is preserved over the entire depth as opposed to conventional imaging.

Ultrafast imaging has already been exploited to measure the dissolution of microbubbles at frame rates of 250 Hz [19], the formation of bubbles from gas precursors during drug delivery [20], and the super-localization of microbubbles [21]. Interestingly for microbubble imaging, in plane wave compound imaging, each part of the imaged volume is subjected to a large number of pulses at low acoustic amplitude, rather than one pulse at high peak pressure in conventional imaging. Because the destabilization of microbubbles is linked to their relative expansion and compression during insonification [11], contrast agents should be less prone to destruction at lower acoustic amplitudes. Designing nonlinear pulse-sequences for plane-wave imaging could therefore drastically reduce bubble disruption and improve the monitoring of their uptake during molecular imaging with ultrasound.

Our objective is to describe new plane wave nonlinear pulse sequences and apply them to a simple *in vitro* model of microbubbles flowing within a wall-less vessel phantom. We first compare the disruption of the microbubbles with focused and plane waves. Then, we shall examine a standard sequence, contrast pulse specific (CPS). **[AU3: CPS is defined elsewhere as contrast pulse sequence. OK to delete? Please check usage of CPS throughout.]** applied to plane wave imaging.

II. METHODS

A wall-less phantom was molded by pouring an agar (3%) gel around a 5-mm-diameter Teflon rod. Cellulose (1%) was added to the agar to obtain a tissue-like appearance on ultrasound images [22]. The resulting tunnel was connected with tubing to a gravity-based flow-system provided by a 1-L container stirred magnetically. Gas-equilibrated water was used as a control [23]. Experimental microbubbles (NA3507, Bracco Suisse SA, Geneva, Switzerland) were prepared as described by the manufacturer,

resulting in a concentration of 2×10^8 bubbles/mL. They were then drawn from the vial with an 18G needle and diluted to a 1/5000 concentration in gas-equilibrated water, before the solution was flowed within the flow-system.

Imaging was performed in a plane perpendicular to the vessel, at 25 mm depth with respect to the transducer-gel interface. The 8-MHz 256-element array was connected to a Supersonic Imagine elastography scanner (Aixplorer, Supersonic Imagine, Aix-en-Provence, France); see Fig. 1. A layer of rubber was added between the array and the gel to attenuate the signal and further reduce bubble disruption. Pulse sequences were programmed on the open ultrasonic system with Matlab (The MathWorks Inc., Natick, MA), giving access to the full emission pattern and beamforming, along with the raw RF data. Pulses were emitted at 7.5 MHz with 33% -6 -dB bandwidth, at a constant pulse rate of 5 kHz for both for plane and focused imaging. The probe was a linear array (256 elements, 200 μ m pitch, 20 mm elevation focus, Vermon, Tours, France). Conventional focused imaging was performed with a single-focus scanned over the 128 lines at $z = 25$ mm depth, with a ratio $f/d = 4$ and at amplitudes varying from 55 to 650 kPa peak negative pressure (PNP). Ultrafast imaging was performed by emitting 121 plane-waves steered from -12° to 12° and beamforming the resulting echoes *a posteriori*. The number of plane waves was defined so that the imaging time, contrast, and resolution would be comparable to that of the conventional focused imaging. The amplitudes of the plane waves, in the same conditions, were 14 to 311 kPa PNP. Prior to the experiment, the pressures emitted by the transducer at 25 mm for the various modes were measured with a calibrated hydrophone (HGL0200, Onda Corp., Sunnyvale, CA).

Plane and focused imaging were modified for nonlinear imaging. Contrast pulse sequence (CPS, [24]) imaging is sensitive to the expansion ratio of a bubble submitted to a pulse of full amplitude and two other pulses of half amplitude (Fig. 2). Nonlinear imaging was performed by interleaving 3 pulses for each emission. First, the odd elements of the array were fired, then a full-amplitude pulse of inverted polarity was emitted, then the even elements of the array were fired (a 3-pulse sequence: $1/2, -1, 1/2$). The CPS was obtained by summing echoes from these three pulses. To control for contrast induced by simple decorrelation of the microbubbles, a sequence was added 4 in which identical pulses were emitted and differentiated. Each imaging sequence consisted of 128×4 (focused) or 121×4 (plane) emissions, which were processed coherently after the acquisition.

For disruption imaging, the flow was stopped for more than 25 s and, then, each imaging sequence was repeated 100 times over the tube, every 0.4 s. The same population of microbubbles was hence submitted to a succession of acoustic waves comparable to those used in molecular imaging with ultrasound. A fresh bolus of 5 mL of microbubbles was injected for each experiment, separated by about 75 s. Both plane waves and focused waves were tested 5 times at each amplitude.

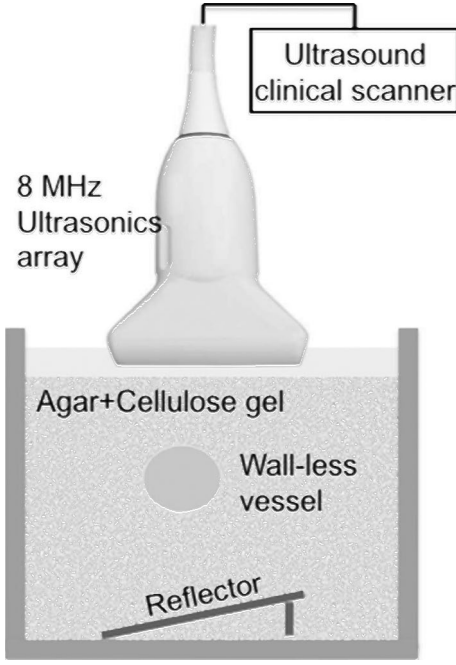


Fig. 1. Setup for the disruption and contrast experiment. Microbubbles are injected through a wall-less vessel, transversal to the plane of imaging. The various pulse sequences are emitted by an 8-MHz transducer array connected to an ultrafast elastography scanner.

Contrast levels were comparable between CPS-focused and plane-wave imaging for microbubbles flowing at 3 mL/min inside the tube. The flow was optimized to reduce artifactual contrast induced by decorrelation and provide fresh microbubbles for each experiment. The two pulse sequences were tested at various amplitudes, in a random order, and the resulting echo from contrast was compared with the echo from the tissue phantom. To determine the CTR, the intensity was averaged over the region around the center of the vessel in the ultrasound image as compared with the average in the tissue phantom at the same depth. The decorrelation signal was tested with the same flow conditions.

III. RESULTS AND DISCUSSIONS

To determine the sensitivity of microbubbles toward the conventional focused pulses and the plane-wave pulses, these two types of imaging were repeated 100 times over a static population of contrast agents. The difference in ultrasound intensity within the wall-less vessel before and after this sequence was considered to be the disruption ratio. As shown in Fig. 3(a), the disruption ratio increased with PNP following an exponential curve ($k_{\text{focused}} = 7.1 \pm 0.8$, $k_{\text{plane}} = 12 \pm 2$). The plateau value, i.e., the point of complete disruption, was 0.99 ± 0.04 for focused waves and 1.05 ± 0.07 for plane waves. The plane-wave sequence disrupted microbubbles in greater number because, at similar PNP, each pixel received 10 times more acoustic energy spread over 121 compounded angles. However, the difference between the two curves remained quite small,

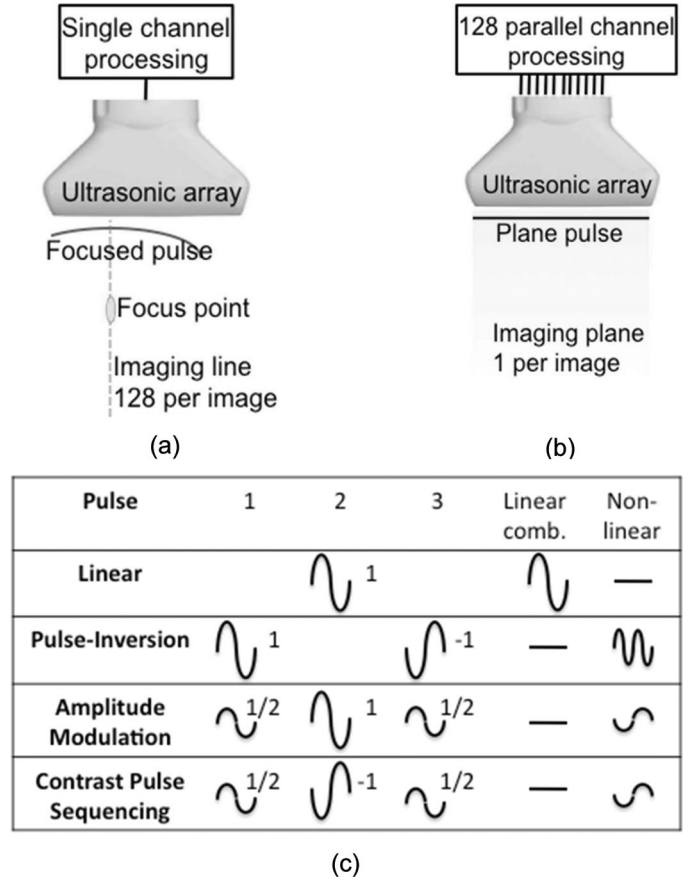


Fig. 2. (a) In conventional focused imaging, ultrasound waves are electronically focused in emission and reception on each line. (b) In plane-wave imaging, the transducer emits a plane wave and the received echoes, collected on all channels in parallel, are beamformed synthetically. Unfocused plane-waves attain lower pressures, but the SNR and contrast are compensated by the emission of multiple plane waves at various angles (compounding). (c) Nonlinear microbubble detection exploits a combination of the ultrasound echoes after the emission of different pulses. Pulse-inversion is the summation of the echoes from two pulses of opposite polarity, which cancels tissue signal responding in a linear fashion. Amplitude modulation is the subtraction of the echoes from one pulse from the summation of the echoes from two half-pulses emitted with a fraction of the transducers. Contrast pulse sequencing (CPS) is a combination of these two techniques. In this paper, focused imaging and plane wave imaging are compared for CPS in which the echoes of the following three pulses are compared: $1/2$, -1 , $1/2$.

demonstrating that the PNP was the main determinant for microbubble disruption. In Fig. 3(b), the same behavior is plotted with respect to the spatial-peak temporal average intensity (I_{SPTA}) impinging on each pixel. Note that the local pressure at $z = 25$ mm corresponds to the elevation focus of the probe. Also note that the exposure of the pixel from neighboring lines is not taken into account for the focused beam intensity measurements. To attain a similar disruption (50%), plane-waves can deposit 24 times more energy than focused waves, highlighting the dominant contribution of the PNP over the total energy. Hence, a single high-pressure pulse (focused) appeared to disrupt more microbubbles than several lower pressure pulses (plane wave).

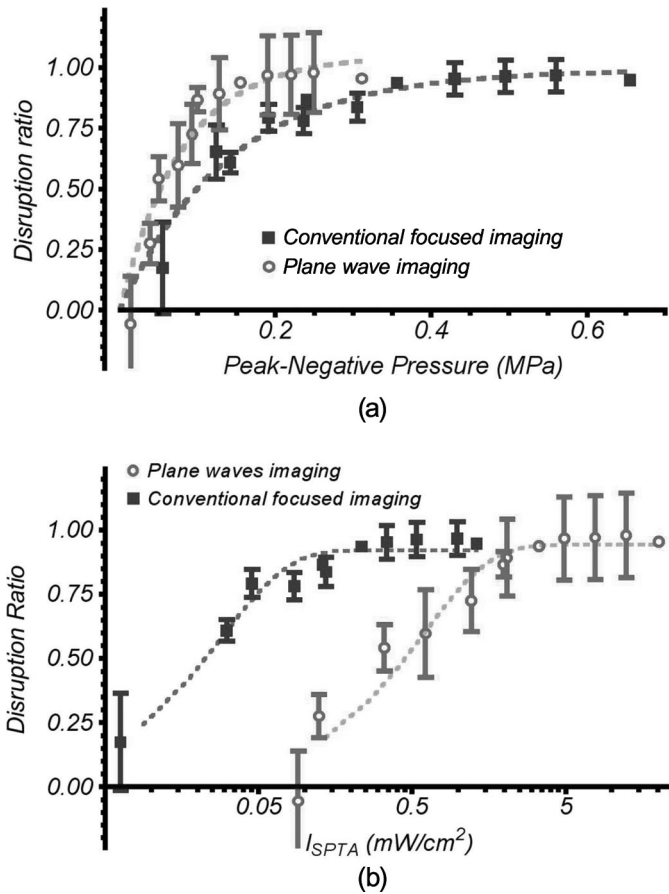


Fig. 3. (a) Disruption ratio after 100 images obtained with conventional focused imaging or plane wave imaging. The ratio is calculated with the intensity of the microbubble echo at the first and last imaging of the full sequence. In plane-wave imaging, each pixel is insonified 121 times rather than a single time in focused imaging. Hence, at the same peak negative pressure (PNP), plane-wave imaging disrupts slightly more bubbles. (b) Disruption ratio as calculated with respect to the total intensity received at each pixel for a single image. Plane-wave imaging spread the energy over more pulses at lower pressure. Because microbubbles are sensitive to the PNP, rather than the total energy, the 50% disruption point is only observed at 0.47 mW/cm² for plane-wave imaging, compared with 0.02 mW/cm² for focused pulses. Less acoustic energy can be emitted with focused pulses before disruption of microbubbles occurs.

For contrast measurements, bubbles were slowly flowed through the wall-less vessel phantom and imaged with conventional focused pulses and plane-waves. Nonlinear detection was performed through combinations of the echoes of the 3 pulses (1/2, -1, 1/2, each separated by 200 μ s), a CPS. In the case of focused imaging, each of these sums represented one nonlinear A-line, which could then be stacked to form a B-mode image. For plane wave imaging, these sums formed one entire nonlinear image obtained at a single angle. The images obtained at different angles were then added coherently to form a compounded plane-wave nonlinear B-mode. In both cases, for plane-wave and conventional imaging, the time between the pulses 1/2, -1, and 1/2 was the same (200 μ s). The images shown in Fig. 4 were taken at low PNPs so that only 25% of the bubbles would be destroyed after 100 images for both plane-wave and focused imaging. For a

concentration of bubbles of 1/5000, the fundamental (linear) imaging displayed a lower contrast within the vessel than in the tissue phantom. As seen in Fig. 4(a) and 4(b), the contrast obtained with 121 compounded planes-waves rather than 128 focused pulses is slightly improved and more homogeneous (plane: -9.6 and focused: -6.9 dB). This enhancement involving less pulses and lower PNP with plane-wave imaging was already observed by Montaldo *et al.* [16]. The border of the vessel appeared to be well defined in both types of imaging, which also had similar spatial frequency content. Other experiments (not shown) also showed that the image of a point scatterer (a 100- μ m wire) was similar between the two imaging techniques. Consequently, the same resolution could be achieved by coherently summing the contribution from compounded angles compared with focused imaging.

CPS is the result of the addition of pulse 2 (full array emitting inverted polarity), to pulse 1 and 3 (even and odd elements). At pressure yielding 25% disruption rate after 100 images, CTR was positive in conventional focused waves. As shown in Fig. 4(d), this contrast method was improved by 11 dB with plane-wave illumination. The vessel containing microbubbles was brighter and more uniform.

The evolution of the average contrast between the vessel and the surrounding tissue phantom with the incident pressure is shown in Fig. 5(a). As previously noted, for a specific PNP, the total incident acoustic energy at any point was much larger with plane-wave imaging because each pixel was insonified 121 times rather than once. The contrast-to-tissue ratio for fundamental imaging was seen to decrease slightly and attained -17 dB for plane wave imaging and -10 dB with conventional focused imaging. Because the bubble concentration was low (1/5000), any improvement in the images was expected to decrease the negative contrast with tissue. CPS applied to conventional focused imaging displayed a regular increase from the low PNP before attaining a peak after 0.3 MPa. This line also represented the pressure at which 90% of the microbubbles would be destroyed after 100 images. Hence, maximum contrast in conventional imaging was only reached when most microbubbles would disappear. The maximum contrast was 13.6 dB for CPS (at 0.30 MPa, 82% disruption rate). However, as described later, part of this contrast was probably a result of decorrelation induced by the motion or disruption of the bubbles at such high pressures.

Nonlinear sequences with plane-wave imaging showed a very different behavior. First, contrast peaked at much lower pressures, 0.05 MPa PNP for CPS. Such pressures corresponded to a lower disruption rate after 100 images; conventional imaging, 82% and plane-wave imaging 50%. CPS reached 16-dB contrast with respect to tissue phantom at 0.05 MPa PNP.

Fig. 5(b) shows the same variations, but with respect to the I_{SPTA} , a measure of the total power impinging on a pixel. Because the acoustic energy deposited at any point is higher with plane-wave imaging, the curve was moved to the right of the graph. Because higher PNPs

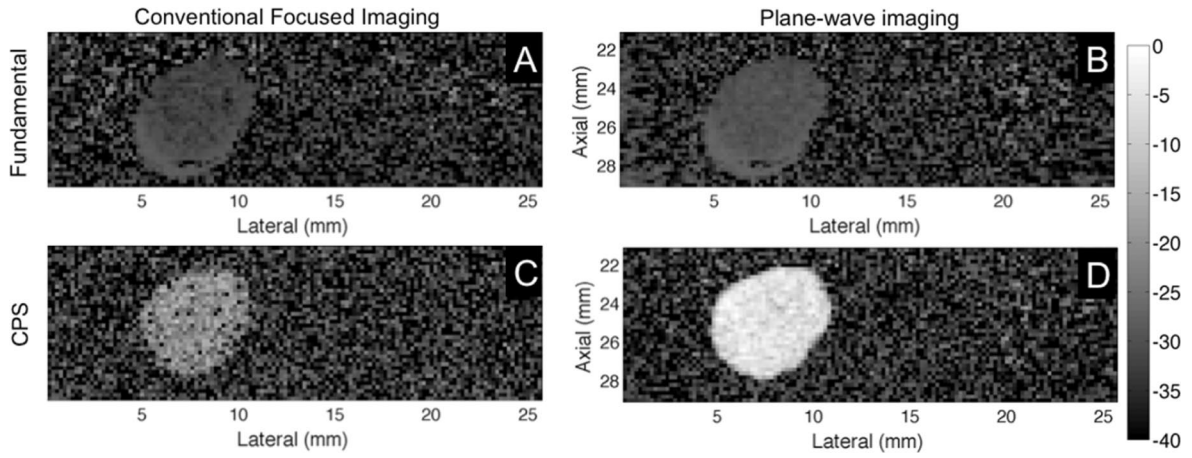


Fig. 4. Image obtained with the 4 pulse-sequences with (left) focused imaging and (right) plane-wave imaging for a similar, 25%, disruption ratio of microbubbles after 100 images (focused: 55 kPa peak negative pressure and plane waves = 40 kPa). The contrast level (40 dB) is normalized to the tissue-phantom on the right of the image and 9 images are averaged. At similar disruption ratio, microbubbles imaged with plane waves are more contrasting than with focused pulse-sequences. Contrast-to-tissue ratio (CTR) for each image: (A) fundamental focused = -6.9 Db, (B) fundamental plane = -9.6 dB, (C) contrast pulse sequencing (CPS) focused = 4.2 dB, (D) CPS plane = 16.7 dB.

were reached with conventional focused imaging, the I_{SPTA} at which 50% bubble disruption is observed was much lower. Both imaging methods clearly displayed a peak in contrast. This maximum is the result of the gain in SNR and the decorrelation of the signal resulting from the motion of the microbubbles and their disruption. The peak was attained when 50% of the microbubbles were destroyed for plane-wave and at a much high disruption rate for conventional focused imaging. Interestingly, the contrast attained in CPS by plane wave imaging appeared to be the continuation of the curve corresponding to conventional focused imaging. Such behavior highlights the fact that contrast is linked to the total energy impinging on the microbubbles. This intensity could be increased significantly with plane wave imaging without inducing rapid disruption, thus resulting in two gain effects on the bubbles contrast: the accumulation of transmitted energy and the reduction of acoustic pressure.

In molecular imaging with ultrasound, an increase in contrast from the microbubbles with respect to tissue must be attained without affecting the survival of the contrast agents to allow a study of the binding dynamic. Fig. 5(c) shows the same CPS contrast, but with respect to the disruption rate of the microbubbles after 100 images. At 50% disruption ratio, plane-wave imaging had 11 dB higher contrast than conventional focused imaging with CPS. The peak contrast for focused imaging was only attained when a high fraction ($>90\%$) of the microbubbles were disrupted.

In multiple pulse sequences imaging, several factors can induce contrast. Ideally, the nonlinear effect from microbubbles can reveal itself through an asymmetry in their compression and expansion phase (pulse-inversion, [25]) or through a disproportionate expansion of the gas with respect to the pressure (amplitude modulation, [4]). However, the contrast-to-tissue ratio can be degraded by the nonlinear scattering from tissue at higher acoustic pres-

ures, requiring compensation techniques [26]. Moreover, additional variations between the echoes of the pulses within the sequence can be induced by the motion of the scatterers or their disruption [27]. These effects are artifactual because they are not truly representing the nonlinearity of the echo of the microbubbles, but rather changes which could also affect other kinds of scatterers such as red blood cells. As a consequence, there is a real gain in combining multiple compounded transmissions at a low pressure level.

To produce Fig. 6, the 3 pulses sequence $(1/2, -1, 1/2)$ was converted to a sequence of 4 identical pulses $(1, 1, 1, 1)$. Differential imaging was implemented by summing the absolute difference of the echoes between each of these images. Such a sequence should have revealed any effect induced by decorrelation, because the absence of motion and disruption should not yield any contrast. As shown in Fig. 7, plane-wave imaging, at any PNP within the range considered, did not induce any decorrelation contrast between the vessel and the surrounding tissue phantom. However, focused pulses caused important variation within the medium because decorrelation CTR increased to 12 dB. Such changes between pulses can be due to fast disruption happening within the 4 pulses-sequence itself or bubble motion induced by the radiation pressure caused by the high intensity attained by single pulses. Because PNP was lower for plane-wave imaging, neither disruption nor radiation push was noticeable. Consequently, plane-wave contrast observed in previous experiments was detected through the nonlinear behavior of bubbles itself, whereas the contrast in conventional focused imaging was a combination of the nonlinearity of the microbubbles and signal decorrelation.

The gain in contrast obtained from plane-wave imaging appeared to be dependent on the increased number of insonifications on each pixel and the spread of a higher acoustic energy over these compounded angles. As shown

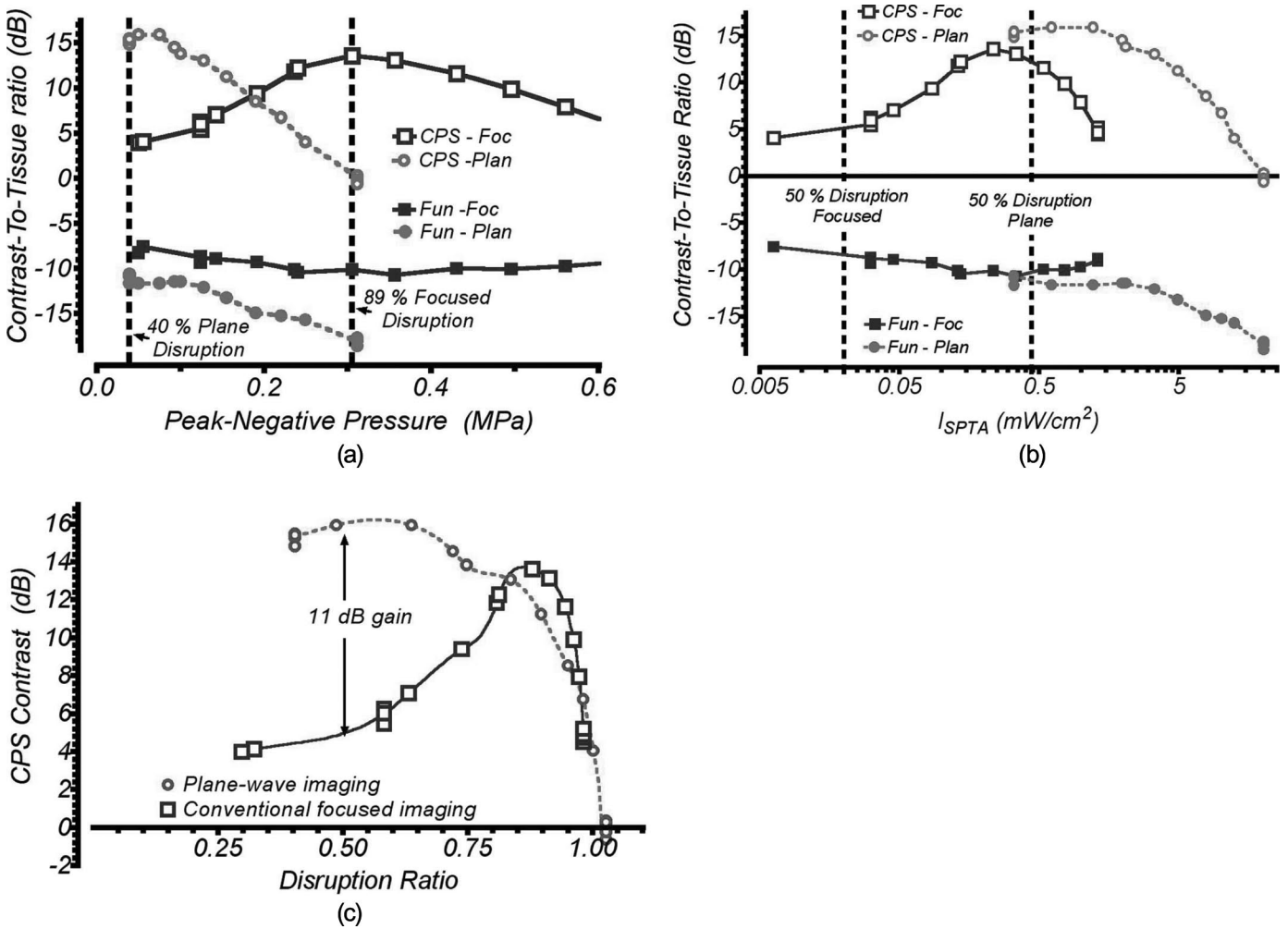


Fig. 5. (a) Summary of the average contrast between the intensity of microbubbles and tissue in the ultrasound image with the 4 pulse sequences. In contrast pulse sequencing (CPS), the highest microbubble contrast is 16.1 dB with respect to tissue with plane waves and 13.7 dB for focused waves. Moreover, at the peak CPS contrast for plane waves, 40% of the bubbles are destroyed, compared with 89% for the peak CPS contrast for focused waves. (b) Average contrast of the intensity of microbubbles and tissue in the ultrasound images with respect to the total energy density deposited on each pixel. Because plane-wave imaging spread the energy on each pixel over multiple compounded pulses of lower peak negative pressure (PNP), the total energy emitted is higher than for focused pulses. This increased intensity allows a higher contrast-to-tissue ratio (CTR), despite a reduced disruption ratio. (c) CTR in CPS for plane wave and focused imaging. To preserve 50% of the bubbles after 100 images, PNP must be reduced in conventional focused imaging and only 5 dB in contrast is observed with respect to the tissue-phantom. At the same disruption ratio, plane-wave imaging attains 16 dB in CTR.

in Fig. 7, the contrast-to-tissue ratio increased linearly with the square root of the number of compounded angles summed to obtain one image. This relationship held true until the further addition of compounded plane-wave angles between the set limits of -12° to 12° caused the measurements to become dependent on each other. For echoes to be independent in these conditions, a minimum difference of 0.5° was required between the angles. Only 5 emissions were necessary to attain the same contrast between plane-wave imaging and conventional focused imaging. Consequently, for equivalent contrast-to-tissue ratio, plane-wave imaging could be performed 25 times faster.

This paper described the implementation of contrast plane wave imaging. The synthetic coherent recombination of such unfocused beams leads to a significant increase in contrast and reduction in microbubble disruption in comparison with conventional contrast imaging using focused

beams. Some parameters were kept constant to allow a fair comparison, such as the frequency or the total number of pulses emitted. Nevertheless, contrast plane-wave imaging could be made significantly faster (up to 5000 images per second) because only a few angles must be summed during coherent compounding to obtain comparable CTR. Such frame rates might appear superfluous for conventional imaging, but they become essential for monitoring the diffusion rate of microbubbles [19], which could provide information on the static pressure or the geometry of the surrounding vessels. Moreover, super-localization imaging of microbubbles, which improves resolution to $6 \mu m$ at 1 MHz [21], also requires very fast frame rates to observe minute changes affecting microbubbles within 1 ms.

Plane-wave imaging can thus attain optimal contrast below 50 kPa, at which the microbubbles are unlikely to disrupt, while retaining a nonlinear behavior [28]. How-

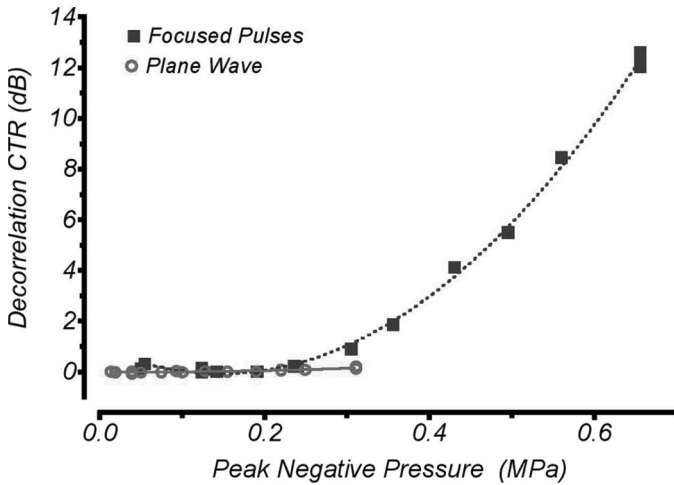


Fig. 6. Effect of the decorrelation of the echo on the microbubble detection. Any motion in the medium between pulses of the same sequence induces a decorrelation artifact, which is independent of the nonlinear nature of the microbubbles. Because agents in solution are both pushed by radiation pressure and rapidly destroyed, such effects can create a false contrast. Four identical pulses were emitted following the same timing as the nonlinear sequences exposed previously. Differential imaging demonstrates that higher pressures induced by focused pulses move and/or destroy microbubbles rapidly and create decorrelation contrast. This artifact is not observed with plane-wave imaging.

ever, we could envision reducing the acoustic pressure even more. Indeed, beamforming can also be performed through the recombination of the echoes obtained from element-by-element emissions [29]. This technique could retrieve similar resolution for pressure levels below 10 kPa, but would not induce nonlinear behavior in microbubbles. In fact, plane-wave imaging lies between two extremes, between the low pressures used in element-by-element imaging and the high pressures used in focused imaging. Fortunately, the pressures used in plane-wave imaging (50 to 100 kPa) also correspond to the proper compromise between nonlinear behavior of the microbubbles and their disruption threshold.

IV. CONCLUSION

Compared with conventional contrast imaging, contrast plane-wave imaging leads to a significant increase of the contrast-to-tissue ratio of contrast-specific sequencing (CPS) at a specific disruption ratio. Such a gain is due to the spread of the acoustic energy over many pulses, thus reducing the maximum peak pressure without compromising the total acoustic energy used. The resulting increase in intensity attained with plane-wave, without bubble disruption, leads to the increase in contrast. Preserving microbubbles and enhancing their detection during long imaging procedures could drastically improve molecular and perfusion imaging. For instance, a constant monitoring of the contrast agents' progression could yield better measurements of total blood volume, flow, attachment efficiency, and ligand affinity. With nonlinear plane-waves im-

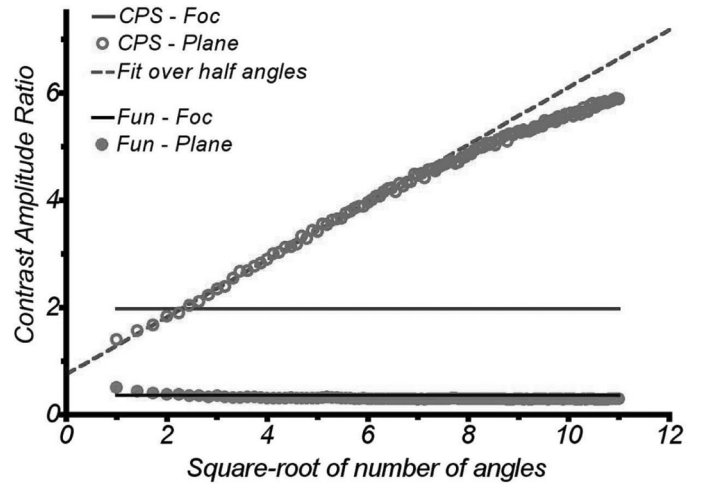


Fig. 7. Contribution of the number of compounded plane waves (angles from -12° to 12°) to the total contrast-to-tissue ratio (in linear amplitude) at 50 kPa peak negative pressure (PNP). To produce a compound plane-wave image, several beamformed images obtained at different angles of insonification are coherently summed. In this case, the contrast increases with the square root of the number of angles ($R^2 = 0.99$) for 40 angles between -12° to 12° . When a higher number of angles was used (less than 0.5° between angles), the resulting images were no longer independent and the contribution of each image to the overall contrast was no longer linear.

aging, ultrasound would still benefit from its exceptionally high frame rate even when performing molecular imaging.

ACKNOWLEDGMENTS

We thank Bracco Research SA for providing the contrast agents.

REFERENCES

- [1] P. Burns and S. Wilson, "Microbubble contrast for radiological imaging: 1. Principles," *Ultrasound Q.*, vol. 22, no. 1, pp. 5–13, 2006.
- [2] N. de Jong, P. Frinking, A. Bouakaz, and F. Ten Cate "Detection procedures of ultrasound contrast agents," *Ultrasonics*, vol. 38, no. 1–8, pp. 87–92, 2000.
- [3] D. H. Simpson, C. T. Chin, and P. N. Burns, "Pulse inversion Doppler: A new method for detecting nonlinear echoes from microbubble contrast agents," *IEEE Trans. Ultrason. Ferroelectr. Freq. Control*, vol. 46, no. 2, pp. 372–382, 1998.
- [4] R. Eckersley, C. Chin, and P. Burns, "Optimising phase and amplitude modulation schemes for imaging microbubble contrast agents at low acoustic power," *Ultrasound Med. Biol.*, vol. 31, no. 2, pp. 213–219, 2005.
- [5] K. Wei, "Contrast echocardiography: Applications and limitations," *Cardiol. Rev.*, vol. 20, no. 1, pp. 25–32, 2012.
- [6] S. R. Wilson and P. N. Burns, "Microbubble contrast for radiological imaging: 2. Applications," *Ultrasound Q.*, vol. 22, no. 1, pp. 15–18, 2006.
- [7] J. R. Lindner, "Molecular imaging of cardiovascular disease with contrast-enhanced ultrasonography," *Nature Rev. Cardiol.*, vol. 6, no. 7, pp. 475–481, 2009.
- [8] I. Tardy, S. Pochon, M. Theraulaz, P. Emmel, L. Passantino, F. Tranquart, and M. Schneider "Ultrasound molecular imaging of VEGFR2 in a rat prostate tumor model using BR55," *Invest. Radiol.*, vol. 45, no. 10, pp. 573–578, 2010.
- [9] J.R. Lindner "Assessment of inflammation with contrast ultrasound," *Prog. Cardiovasc. Dis.*, vol. 44, no. 2, pp. 111–120, 2001.

- [10] J. Hudson, R. Williams, B. Lloyd, M. Atri, T. K. Kim, G. Bjarnason, and P. N. Burns, "Improved flow measurement using microbubble contrast agents and disruption-replenishment: Clinical application to tumour monitoring," *Ultrasound Med. Biol.*, vol. 37, no. 8, pp. 1210–1221, 2011.
- [11] J. Chomas, P. Dayton, J. Allen, K. Morgan, and K. Ferrara, "Mechanisms of contrast agent destruction," *IEEE Trans. Ultrason. Ferroelectr. Freq. Control*, vol. 48, no. 1, pp. 232–248, 2001.
- [12] C. Yeh and S. Su, "Effects of acoustic insonation parameters on ultrasound contrast agent destruction," *Ultrasound Med. Biol.*, vol. 34, no. 8, pp. 1281–1291, 2008.
- [13] L. Sandrin, M. Tanter, S. Catherline, and M. Fink, "Shear modulus imaging with 2-D transient elastography," *IEEE Trans. Ultrason. Ferroelectr. Freq. Control*, vol. 49, no. 4, pp. 426–435, 2002.
- [14] M. Tanter, J. Bercoff, L. Sandrin, and M. Fink, "Ultrafast compound imaging for 2-D motion vector estimation: Application to transient elastography," *IEEE Trans. Ultrason. Ferroelectr. Freq. Control*, vol. 49, no. 10, pp. 1363–1374, 2002.
- [15] J. Bercoff, M. Tanter, and M. Fink, "Supersonic shear imaging: A new technique for soft tissue elasticity mapping," *IEEE Trans. Ultrason. Ferroelectr. Freq. Control*, vol. 51, no. 4, pp. 396–409, 2004.
- [16] G. Montaldo, M. Tanter, J. Bercoff, N. Benech, and M. Fink, "Coherent plane-wave compounding for very high frame rate ultrasonography and transient elastography," *IEEE Trans. Ultrason. Ferroelectr. Freq. Control*, vol. 56, no. 3, pp. 489–506, 2009.
- [17] J. Bercoff, G. Montaldo, T. Loupas, D. Savery, F. Meziere, M. Fink, and M. Tanter, "Ultrafast compound Doppler imaging: Providing full blood flow characterization," *IEEE Trans. Ultrason. Ferroelectr. Freq. Control*, vol. 58, no. 1, pp. 134–147, 2011.
- [18] E. Mace, G. Montaldo, I. Cohen, M. Baulac, M. Fink, and M. Tanter, "Functional ultrasound imaging of the brain," *Nat. Methods*, vol. 8, no. 8, pp. 662–664, 2011.
- [19] O. Couture, S. Bannouf, G. Montaldo, J. F. Aubry, M. Fink, and M. Tanter, "Ultrafast imaging of ultrasound contrast agents," *Ultrasound Med. Biol.*, vol. 35, no. 11, pp. 1908–1916, 2009.
- [20] O. Couture, M. Faivre, N. Pannacci, A. Babataheri, V. Servois, P. Tabeling, and M. Tanter, "Ultrasound internal tattooing," *Med. Phys.*, vol. 38, no. 2, pp. 1116–1123, 2011.
- [21] O. Couture, B. Besson, G. Montaldo, M. Fink, and M. Tanter, "Microbubble ultrasound super-localization imaging (MUSLI)," in *IEEE Int. Ultrasonics Symp.*, 2011, pp. 1285–1287.
- [22] E. Franceschini, F. T. H. Yu, F. Destrempes, and G. Cloutier, "Ultrasound characterization of red blood cell aggregation with intervening attenuating tissue-mimicking phantoms," *J. Acoust. Soc. Am.*, vol. 127, no. 2, pp. 1104–1115, 2010.
- [23] P. D. Bevan, R. Karshafian, E. G. Tickner, and P. N. Burns, "Quantitative measurement of ultrasound disruption of polymer-shelled microbubbles," *Ultrasound Med. Biol.*, vol. 33, no. 11, pp. 1777–1786, 2007.
- [24] P. Phillips and E. Gardner, "Contrast-agent detection and quantification," *Eur. Radiol. Suppl.*, vol. 9, pp. 4–10, 2004.
- [25] D. H. Simpson, C. T. Chin, and P. N. Burns, "Pulse inversion Doppler: A new method for detecting nonlinear echoes from microbubble contrast agents," *IEEE Trans. Ultrason. Ferroelectr. Freq. Control*, vol. 46, no. 2, pp. 372–382, 1999. **[AU4: This reference appears to be a duplicate of ref 3. Please check list and correct references, delete duplicates, and renumber references as needed.]**
- [26] O. Couture, J. F. Aubry, G. Montaldo, M. Tanter, and M. Fink, "Suppression of tissue harmonics for pulse-inversion contrast imaging using time reversal," *Phys. Med. Biol.*, vol. 53, no. 19, pp. 5469–5480, 2008.
- [27] H. J. Vos, F. Guidi, E. Boni, and P. Tortoli, "Method for microbubble characterization using primary radiation force," *IEEE Trans. Ultrason. Ferroelectr. Freq. Control*, vol. 54, no. 7, pp. 1333–1345, 2007.
- [28] N. de Jong, M. Emmer, C. T. Chin, A. Bouakaz, F. Mastik, D. Lohse, and M. Versluis, "Compression-only behaviour of phospholipid-coated contrast agents," *Ultrasound Med. Biol.*, vol. 33, no. 4, pp. 653–656, 2007.
- [29] M. Karaman, P. C. Li, and M. O'Donnell, "Synthetic aperture imaging for small scale systems," *IEEE Trans. Ultrason. Ferroelectr. Freq. Control*, vol. 42, no. 3, pp. 429–442, 1995.



Olivier Couture was born in Quebec City, Canada, in 1978. He received his B.Sc degree in physics from McGill University, Montreal, Canada, in 2001, and his Ph.D degree from the Department of Medical Biophysics, University of Toronto, Canada, in 2007. After a postdoctoral fellowship at ESPCI in Paris, France, he was hired as a tenured research associate at CNRS, based within the Langevin Institute. He is the author of 12 peer-reviewed articles and 5 patents. His current research interests include drug delivery, ultrasound tattooing, ultrasound contrast agents, HIFU, microfluidics, nonlinear acoustics, and Rayleigh waves in swimming pools.



Mathias Fink received the M.S. degree in mathematics from Paris University, France, in 1967, and the Ph.D. degree in solid-state physics in 1970. He then moved to medical imaging and received the Doctorat es-Sciences degree in 1978 from Paris University. His Doctorat es-Sciences research was in the area of ultrasonic focusing with transducer arrays for real-time medical imaging.

Mathias Fink is a professor of physics at the Ecole Supérieure de Physique et de Chimie Industrielles de la Ville de Paris (ESPCI ParisTech), Paris, France. In 1990, he founded the Laboratory Ondes et Acoustique at ESPCI that became, in 2009, the Langevin Institute. In 2002, he was elected to the French Academy of Engineering, in 2003 to the French Academy of Science, and in 2008 to the College de France on the Chair of Technological Innovation.

Mathias Fink's area of research is concerned with the propagation of waves in complex media and the development of numerous instruments based on this basic research. His current research interests include time-reversal in physics, super-resolution, metamaterials, medical ultrasonic imaging, ultrasonic therapy, multiwave imaging, acoustic smart objects, acoustic tactile screens, underwater acoustics, geophysics, and telecommunications. He has developed different techniques in medical imaging (ultrafast ultrasonic imaging, transient elastography, and supersonic shear imaging), wave control, and focusing in complex media with time-reversal mirrors. He holds more than 55 patents and he has published more than 350 peer-reviewed papers and book chapters. Four start-up companies have been created from his research (Echosens, Sensitive Object, Supersonic Imagine, and Time Reversal Communications)



Mickael Tanter was born in December 1970 in Paimpol, France. He is a Research Professor of the French National Institute for Health and Medical Research (INSERM). For five years, he has headed the team Inserm U979 "Wave Physics for Medicine" at Langevin Institute (CNRS UMR 7587), ESPCI ParisTech, France. In 1999, he was awarded the Ph.D. degree in physics from Paris VII University. His main activities are centered on the development of new approaches in wave physics for medical imaging and therapy. His current research interests cover a wide range of topics: elastography using shear wave imaging, high-intensity focused ultrasound, ultrasonic imaging using ultrafast ultrasound scanners, adaptive beamforming, and combination of ultrasound with optics and MRI. In 2009, he received the Frederic Lizzi Early Career Award of the International Society of Therapeutic Ultrasound. In 2010, he received the Brillouin prize of the SEE and IEEE societies and the Montgolfier prize of the French National Society for Industry Valorization (S.E.I.N.). He is the recipient of 17 patents in the field of ultrasound imaging and the author of more than 80 technical peer-reviewed papers and book chapters. In 2005, M. Tanter, along with M. Fink, J. Souquet, and C. Cohen-Bacrie, founded Supersonic Imagine, an innovative French company positioned in the field of medical ultrasound imaging and therapy that in 2009 launched a new-generation ultrasound imaging platform called Aixplorer with a unique shear wave imaging modality.

search interests cover a wide range of topics: elastography using shear wave imaging, high-intensity focused ultrasound, ultrasonic imaging using ultrafast ultrasound scanners, adaptive beamforming, and combination of ultrasound with optics and MRI. In 2009, he received the Frederic Lizzi Early Career Award of the International Society of Therapeutic Ultrasound. In 2010, he received the Brillouin prize of the SEE and IEEE societies and the Montgolfier prize of the French National Society for Industry Valorization (S.E.I.N.). He is the recipient of 17 patents in the field of ultrasound imaging and the author of more than 80 technical peer-reviewed papers and book chapters. In 2005, M. Tanter, along with M. Fink, J. Souquet, and C. Cohen-Bacrie, founded Supersonic Imagine, an innovative French company positioned in the field of medical ultrasound imaging and therapy that in 2009 launched a new-generation ultrasound imaging platform called Aixplorer with a unique shear wave imaging modality.